Tetrakis([5]trovacenyl)tin: Synthesis, Structure, and Intramolecular Communication†

Christoph Elschenbroich,*,‡ Feng Lu,‡ Mathias Nowotny,§ Olaf Burghaus,‡ Clemens Pietzonka,‡ and Klaus Harms‡

Fachbereich Chemie, Philipps-Universität, 35032 Marburg, Germany, and Eduard-Zintl-Institut für Anorganische und Physikalische Chemie, Technische Universität Darmstadt, 64287 Darmstadt, Germany

Received March 29, 2007

In order to study intermetallic interactions in a tetranuclear complex with tetrahedral disposition of paramagnetic central metal atoms, the organometallic tetraradical $[(\eta^7\text{-}C_7H_7)V(\eta^5\text{-}C_5H_4)]_4Sn$ (**3**$^{4\bullet}$), tetra([5]trovacenyl)tin, was prepared, characterized by X-ray diffraction, and subjected to EPR spectroscopy, magnetic susceptometry, and cyclic voltammetry. The binuclear complex $[(\eta^7\text{-}C_7H_7)V(\eta^5\text{-}C_5H_4)]_2Ph_2Sn$ (**4**$^{2\bullet}$) was also obtained to serve as a reference molecule. The EPR hyperfine pattern attests to exchange coupling which approaches the fast exchange limit, i.e., J_{EPR} (**3**$^{4\bullet}$) $\gg a(^{51}V) = 0.0067$ cm^{-1}. For the dinuclear complex simulation afforded the value $|J(\mathbf{4}^{2\bullet})| = 1.4$ cm^{-1}; magnetic susceptometry yielded the exchange coupling constant $J_\chi(\mathbf{4}^{2\bullet}) = -1.78$ cm^{-1}. No quantitative data could be derived for the tetranuclear complex; however, the gradation $J(\mathbf{3}^{4\bullet}) < J(\mathbf{4}^{2\bullet})$ applies. This may be a result of competing interactions of opposite sign or of spin frustration, as has been discussed previously for tetrahedral spin clusters of the Werner type. Redox splittings for tetrakis([5]trovacenyl)tin are smaller than those for tetrakis(ferrocenyl)silicon.

Introduction

The paramagnetic unsymmetrical sandwich complex (η^7-C_7H_7)V(η^5-C_5H_5) (**1**$^\bullet$; *tro*pylium−*va*nadium−*c*yclop*en*tadi*e*nyl, *trovacene*) offers favorable EPR and redox characteristics[2] as well as comparative ease of derivatization via peripheral substitution. Therefore, trovacene in our hands has been used extensively in the synthesis of oligonuclear paramagnetic organometallics, with the aim of studying spacer-dependent intramolecular electro- and magnetocommunication.[3] Whereas in this endeavor hydrocarbon-based spacers have dominated,[4] boron-[5] and silicon-containing[6] groups have also been interspersed between trovacene units. Group 14 spacer atoms can potentially accommodate up to four trovacenyl units, thereby offering the chance to study electro- and magnetocommunication between sandwich units which are fixed in a tetrahedral disposition. Surprisingly, with the exception of tetrakis(ferrocenyl)silicon, $[(\eta^5\text{-}C_5H_5)Fe(\eta^5\text{-}C_5H_4)]_4Si$ (**2**),[7] compounds of the composition (metallocenyl)$_4$E (E = group 14 element) have not been forthcoming; in this statement, the term "metallocenyl" also encompasses the bis(arene)metal series. We here describe the synthesis and properties of tetrakis([5]-trovacenyl)tin (**3**$^{4\bullet}$).[8] This unprecedented organometallic tetraradical complements paramagnetic inorganic clusters, in which the open-shell metal ions assume tetrahedral positions bridged over the edges by halide ions and possessing a central oxygen atom, $M_4OX_6L_4$ (X = Cl, Br; L = Cl, Br, pyridine, R_3PO, amine N-oxide, R_3NO, etc.),[9] as well as heterocubane-like species with $[M_4L_4L'_4]^{n+}$ cores in which the faces of the M_4 tetrahedra are bridged by groups μ_3-L (L = OR, SR) and the metal ions carry additional terminal ligands L′.[10] In the realm of organic chemistry, while a few tetraradicals have been described,[11] chain-like and cyclic molecular structures predominate and the tetrahedral disposition of the paramagnetic centers is exceptional.[12] Not surprisingly, the most extensive class of organic tetraradicals features pyrrolinyl-1-oxyls and piperidinyl-1-oxyls as spin-bearing units.[13] All of these systems have been studied with the aim of deriving magnetostructural correlations and of gaining information on magnetic exchange mechanisms. Of more practical concern was and is the construction of high-temperature molecular ferromagnets.[14]

* To whom correspondence should be addressed. E-mail: eb@chemie.uni-marburg.de.

† Trovacene Chemistry. 14. Part 13: ref 1.

‡ Philipps-Universität.

§ Technische Universität Darmstadt.

(1) Elschenbroich, C.; Plackmeyer, J.; Harms, K.; Burghaus, O.; Pebler, J. *Z. Anorg. Allg. Chem.* **2006**, *632*, 819.

(2) Elschenbroich, C.; Bilger, E.; Metz, B. *Organometallics* **1991**, *10*, 2823.

(3) Elschenbroich, C.; Schiemann, O.; Burghaus, O.; Harms, K. *Chem. Commun*. **2005**, 2149 and previous papers in the series Trovacene Chemistry.

(4) (a) Schiemann, O.; Plackmeyer, J.; Fritscher, J.; Pebler, J.; Elschenbroich, C. *Appl. Magn. Reson.* **2004**, *26*, 171. (b) Elschenbroich, C.; Plackmeyer, J.; Nowotny, M.; Harms, K.; Pebler, J., Burghaus, O. *Inorg. Chem.* **2005**, *44*, 955. (c) Elschenbroich, C.; Plackmeyer, J.; Nowotny, M.; Behrendt, A.; Harms, K.; Pebler, J.; Burghaus, O. *Chem. Eur. J.* **2005**, *11*, 7427.

(5) Elschenbroich, C.; Wolf, M.; Burghaus, O.; Harms, K.; Pebler, J. *Eur. J. Inorg. Chem*. **1999**, 2173.

(6) (a) Elschenbroich, C.; Bretschneider-Hurley, A.; Hurley, J.; Massa, W.; Wocadlo, S.; Pebler, J. *Inorg. Chem.* **1993**, *32*, 5421. (b) Elschenbroich, C.; Bretschneider-Hurley, A.; Hurley, J.; Behrendt, A.; Massa, W.; Wocadlo, S.; Reijerse, E. *Inorg. Chem*. **1995**, *34*, 743.

(7) MacLachlan, M. J.; Lough, A. J. Geiger, W. E.; Manners, I. *Organometallics* **1998**, *17*, 1873.

(8) The number in brackets indicates the site of substitution: [5]-trovacenyl is functionalized at the cyclopentadienyl ligand and [7]trovacenyl at the cycloheptatrienyl ligand.

(9) (a) Ginsberg, A. P. *Inorg. Chim. Acta Rev*. **1971**, *5*, 45. (b) Lines, M. E.; Ginsberg, A. P.; Martin, R. L.; Sherwood, A. C. *J. Chem. Phys*. **1972**, *57*, 1. (c) Hatfield, W. E.; Barnes, J. A.; Inman, G. W.; *Inorg. Chem*. **1971**, *10*, 1725. (d) Rubins, R. S.; Black, T. D.; Barak, J. *J. Chem. Phys*. **1986**, *85*, 3770. (e) Jones, D. H.; Sams, J. R.; Thompson, R. C. *Inorg. Chem*. **1983**, *22*, 1399. (f) Wong, H.; tom Dieck, H.; O'Connor, C. J.; Sinn, E. *J. Chem. Soc., Dalton Trans.* **1980**, 786.

10.1021/om700300j CCC: $37.00
Publication on Web 06/26/2007

Scheme 1

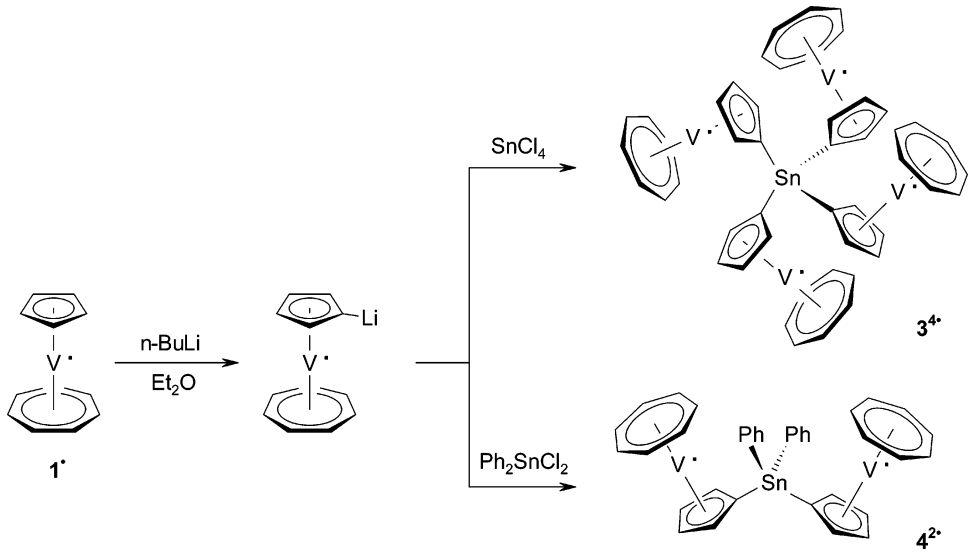

Results and Discussion

The pentanuclear complex $\mathbf{3}^{4\bullet}$ and the trinuclear reference molecule $\mathbf{4}^{2\bullet}$ were prepared by simple Wurtz coupling (Scheme 1).

Molecular Structures. Both $\mathbf{3}^{4\bullet}$ and $\mathbf{4}^{2\bullet}$ were characterized by X-ray diffraction; the molecular structures are depicted in Figures 1 and 2, respectively, and selected bond lengths and angles are collected in the captions.

The unit cell of $\mathbf{3}^{4\bullet}$ contains two pairs of independent molecules with significantly differing structural parameters and deviations from ideal tetrahedral core symmetry: intramolecular nonbonded intervanadium distances in the crystal encompass a range of 6.4 ± 0.4 Å, and the $C_{ipso}-Sn-C_{ipso}$ angles vary between 104 and 114°. Furthermore, the dihedral angles between individual pairs of tin connected cyclopentadienyl ligands vary between 30.0 and 79.4° (see the Supporting Information), which is expected to modulate the contribution of the π-mediated path of magnetic coupling to the total J values.

Conceivably, these distortions are caused by packing effects,

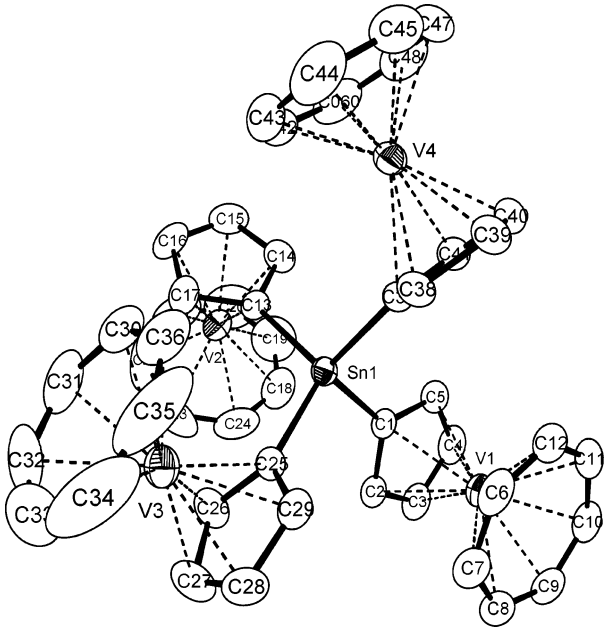

Figure 1. Molecular structure of tetrakis([5]trovacenyl)tin) ($\mathbf{3}^{4\bullet}$) in the crystal (50% probability ellipsoids). One of the two forms present in the unit cell is shown here (see the Supporting Information). Selected bond lengths (Å) and angles (deg): Sn1−C1 = 2.129(2), Sn1−C13 = 2.132(2), Sn1−C25 = 2.128(2), Sn1−C37 = 2.129(2), C1−Sn1−C13 = 108.11(8), C1−Sn1−C25 = 105.66(8), C1−Sn1−C37 = 107.26(9), C13−Sn1−C25 = 113.26-(9), C13−Sn1−C37 = 108.54(8), C25−Sn1−C37 = 113.68(9), V1···V2 = 6.6270(6), V1···V3 = 6.7041(6), V1···V4 = 6.5326-(7), V2···V3 = 6.2384(6), V2···V4 = 6.5204(7), V3···V4 = 6.1288(6), Sn2−C49 = 2.123(2), Sn2−C61 = 2.125(2), Sn2−C73 = 2.123(2), Sn2−C85 = 2.125(2), C49−Sn2−C61 = 108.80(8), C49−Sn2−C73 = 113.54(10), C49−Sn2−C85 = 111.79(8), C61−Sn2−C73 = 104.55(9), C61−Sn2−C85 = 107.49(9), C73−Sn2−C85 = 110.24(9), V5···V6 = 6.6660(6), V5···V7 = 6.2817(6), V5···V8 = 6.5894(6), V6···V8 = 6.4964(6), V6···V7 = 6.8311-(7), V7···V8 = 6.0536(8).

(10) (a) Ginsberg, A. P.; Bertrand, J. A.; Kaplan, R. I.; Kirkwood, C. E.; Martin, R. L.; Sherwood, R. C. *Inorg. Chem.* **1971**, *10*, 240. (b) Merz, L.; Haase, W. *J. Chem. Soc., Dalton Trans.* **1978**, 1594. (c) Laurent, J.-P.; Bonnet, J.-J.; Nepveu, F.; Astheimer, H.; Walz, L.; Haase, W. *J. Chem. Soc., Dalton Trans.* **1982**, 2433. (d) Schwabe, L.; Haase, W. *J. Chem. Soc., Dalton Trans*. **1985**, 1909. (e) Hall, J. W.; Estes, W. E.; Estes, E. D.; Scaringe, R. P.; Hatfield, W. E. *Inorg. Chem*. **1977**, *16*, 1572. (f) Taft, K. L.; Caneschi, A.; Pence, L. E.; Delfs, C. D.; Papaefthymion, G. C.; Lippard, S. J. *J. Am. Chem. Soc.* **1993**, *115*, 11753. (g) Ruiz, E.; Rodríguez-Fortia, A.; Alemany, P.; Alvarez, S. *Polyhedron* **2001**, *20*, 1323. (h) Yoo, S. J.; Angove, H. C.; Burgess, B. K.; Hendrich, M. P.; Münck, E. *J. Am. Chem. Soc.* **1999**, *121*, 2534. (i) Oshio, H.; Hoshino, N.; Ito, T.; Nakano, M. *J. Am. Chem. Soc.* **2004**, *126*, 8805. (j) Oshio, H.; Hoshino, N.; Ito, T. *J. Am. Chem. Soc.* **2000**, *122*, 12602. (k) Clemente-Juan, J. M; Mackiewicz, C.; Verelst, M.; Dahan, F.; Bousseksou, A.; Sanakis, Y.; Tuchagues, J.-P. *Inorg. Chem.* **2002**, *41*, 1478. (l) Rajaraman, G.; Christensen, K. E.; Larsen, F. K.; Timco, G. A.; Winpenny, R. E. P. *Chem. Commun.* **2005**, 3053. (m) Bencini, A.; Gatteschi, D.; Zanchini, C.; Haasnoot, J. G.; Prins, R.; Reedijk, J. *J. Am. Chem. Soc.* **1987**, *109*, 2926. (n) Bencini, A.; Gatteschi, D. *EPR of Exchange Coupled Systems*; Springer: Berlin, 1990; pp 113−120.

(11) (a) Ferruti, P.; Gill, D.; Klein, M. P.; Wang, H. W.; Entine, G.; Calvin, M. *J. Am. Chem. Soc.* **1970**, *92*, 3704. (b) Rajca, A. *Chem. Rev.* **1994**, *94*, *871*. (c) Nau, W. M. *Angew. Chem., Int. Ed. Engl.* **1997**, *36*, 2445.

(12) (a) Nakajima, A.; Ohya-Nishiguchi, H.; Deguchi, Y. *Bull. Chem. Soc. Jpn*. **1971**, *44*, 2120. (b) Kopf, P. W.; Kreilick, R. W.; Boocock, D. G. B.; Ullman, E. F. *J. Am. Chem. Soc.* **1970**, *92*, 4531. (c) Liao, Y.; Baskett, M.; Lahti, P. M.; Palacio, F. *Chem. Commun.* **2002**, 252.

(13) Amabilino, D. B.; Veciana, J. In *Magnetism: Molecules to Materials II*; Miller, J. S., Drillon, M., Eds.; Wiley-VCH: Weinheim, Germany, 2001; Chapter 1.

(14) (a) Kahn, O. *Molecular Magnetism*; VCH: Weinheim, Germany, 1992. (b) Miller, J. S.; Drillon, M. *Magnetism: Molecules to Materials I-V*; Wiley-VCH: Weinheim, Germany, 2001. (c) Iwamura, H., Inoue, K.; Hayamizu, T. *Pure Appl. Chem.* **1996**, *68*, 243. (d) Verdaguer, M. *Polyhedron* **2001**, *20*, 1115. (e) Gatteschi, D. *Adv. Mater.* **1994**, *6*, 635. (f) Miller, J. S.; Epstein, A. J. *Angew. Chem., Int. Ed. Engl.* **1994**, *33*, 385.

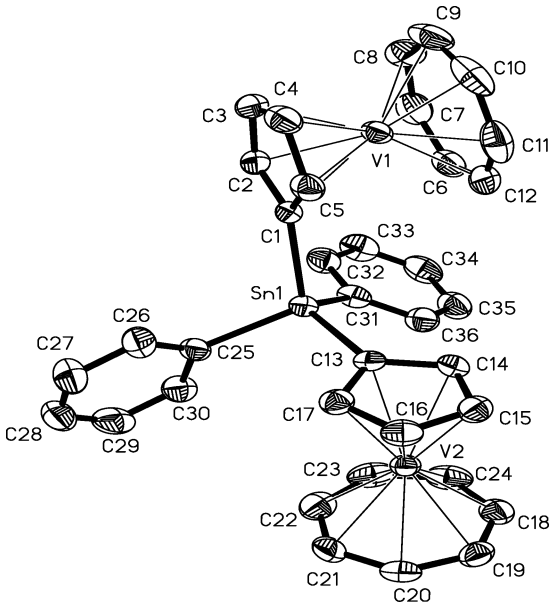

Figure 2. Molecular structure of bis([5]trovacenyl)diphenyltin (**4**$^{2\bullet}$) in the crystal (50% probability ellipsoids). Selected bond lengths (Å) and angles (deg): Sn1−C1 = 2.132(2), Sn1−C13 = 2.121(2), Sn1−C25 = 2.137(2), Sn1−C31 = 2.138(2), C1−Sn1−C13 = 107.60(8), C1−Sn1−C25 = 108.20(8), C1−Sn1−C31 = 107.13-(8), C13−Sn1−C25 = 106.09(9), C13−Sn1−C31 = 114.30(9), C25−Sn1−C31 = 113.26(9), V1···V2 = 6.961(2).

and in fluid solution molecules of **3**$^{4\bullet}$ will relax to a more symmetrical structure. In the diradical complex **4**$^{2\bullet}$ the intervanadium distance of 6.96 Å slightly exceeds the mean value in **3**$^{4\bullet}$; presumably the less encumbered tin environment tolerates a conformation in which the trovacenyl units maximize their separation. The dimensions of the trovacenyl units differ only insignificantly from those of the parent molecule **1**$^{\bullet}$.[15]

EPR Spectra. EPR spectra of **4**$^{2\bullet}$ (Figure 3) and **3**$^{4\bullet}$ (Figure 4) in fluid solution exhibit ^{51}V hyperfine structures which approach the fast exchange limit ($J \gg a(^{51}\mathrm{V}, \mathbf{1}^{\bullet}) = 0.0067$ cm^{-1}, $I(^{51}\mathrm{V}) = {}^{7}/_{2}$), as inferred from the observation of 15 lines (**4**$^{2\bullet}$, spacing $a(^{51}\mathrm{V}, \mathbf{1}^{\bullet})/2$) and 29 lines (**3**$^{4\bullet}$, spacing $a(^{51}\mathrm{V}, \mathbf{1}^{\bullet})/4$), respectively. Simulation of the spectrum of the diradical **4**$^{2\bullet}$ yielded the value $|J_{\mathrm{EPR}}(\mathbf{4}^{2\bullet})| = 1.4$ cm^{-1}, which is markedly smaller than that for the methylene-spacered complex bis([5]-trovacenyl)methane ($|J_{\mathrm{EPR}}(\mathbf{5}^{2\bullet})| > 1.5$ cm^{-1}, $J_{\chi} = -4.25$ cm^{-1}).[4c] Since a computer program to simulate the hyperfine structure of exchange-coupled tetraradicals such as **3**$^{4\bullet}$ does not appear to be available, the qualitative conclusion that **3**$^{4\bullet}$ is extensively exchange coupled must suffice. In any case, the hyperfine pattern in **3**$^{4\bullet}$ is not resolved sufficiently well to invest intensive efforts at its simulation. The rigid solution spectra of **3**$^{4\bullet}$ and **4**$^{2\bullet}$ point to *g* anisotropy, zero-field splitting, and exchange coupling of similar magnitude, rendering unambiguous analysis impractical.

Magnetic Susceptibility. For oligoradicals which are built from monoradicals with a central metal hyperfine coupling constant of the order displayed by **1**$^{\bullet}$ ($a(^{51}\mathrm{V}) = 7.18$ mT ≙ 0.0067 cm^{-1}), analysis of the hyperfine pattern and magnetic susceptibility measurements are complementary in that the former is noticeably influenced if $J \lesssim 200[a(^{51}\mathrm{V})] \approx 1.4$ cm^{-1}, while the latter is applicable for $J \gtrsim 1$ cm^{-1}. We therefore recorded the temperature dependence of magnetic susceptibilities for **3**$^{4\bullet}$ and **4**$^{2\bullet}$; the respective traces are shown in Figures 5 and 6. The magnetic behavior of the diradical **4**$^{2\bullet}$ is straightforward in that a maximum of the $\chi_{\mathrm{m}}-T$ curve appears near 2.56 K, which attests to weak antiferromagnetic coupling. Fitting this susceptibility curve by means of the modified Bleaney−Bowers formula yielded the value $J_{\chi}(\mathbf{4}^{2\bullet}) = -1.78$ cm^{-1} ($\Theta = -3.1$ K

$$\chi = (2Ng^2\mu_{\mathrm{B}}{}^2/3k(T-\Theta))[1 + {}^{1}/_{3}\exp(-J/kT)]^{-1}$$

corrects for intermolecular antiferromagnetic interaction). The exchange coupling constant J_{χ} (**4**$^{2\bullet}$) is considerably smaller than $J_{\chi}(\mathbf{5}^{2\bullet}) = -4.25$ cm^{-1} for bis([5]trovacenyl)methane (**5**$^{2\bullet}$),[4c] where a $-CH_2-$ rather than a $-SnPh_2-$ unit serves as a spacer. The magnetic susceptibility results thereby confirm the gradation of J_{EPR} inferred from the isotropic EPR spectra of **4**$^{2\bullet}$ and **5**$^{2\bullet}$.

Surprisingly, a perfect fit of the $\chi-T$ curve for the tetraradical **3**$^{4\bullet}$ was achieved by applying the simple Curie−Weiss law (Figure 6). Therefore, no quantitative information on the type and magnitude of the exchange interaction can be extracted from this trace, at least in the accessible temperature range. This finding must be discussed on the basis of the magnetic behavior of tetrahedral $4 \times S = {}^{1}/_{2}$ species alluded to in the Introduction. A common feature of these tetraradicals is the presence of competing interactions which may even be of opposite sign depending on the coupling path, its chemical nature, and its geometrical characteristics.[9a,c,e,f,10b−d,i,k] The latter is demonstrated by the sensitive response of *J* to changes in the M−O−M bridge angle in hydroxy- and phenoxy-bridged paramagnetic dinuclear complexes.[10h,16] For a series of hydroxo-bridged Cu-(II) complex dimers, *J* values between +86 and −255 cm^{-1} for Cu−O−Cu angles in the range from 95.6 to 104.1° have been determined.[16a] As for tetrakis([5]trovacenyl)tin (**3**$^{4\bullet}$) the $C_{ipso}-Sn-C_{ipso}$ angles cover a similar range, it is conceivable that competing ferro- and antiferromagnetic contributions cancel to a large extent and the experimental $\chi-T$ curve fails to reflect intramolecular exchange coupling.

An alternative rationalization which neglects the deviations from ideal tetrahedral symmetry for **3**$^{4\bullet}$ is based on the phenomenon of spin frustration. Herein it is assumed that all six pairwise exchange interactions in **3**$^{4\bullet}$ are inherently antiferromagnetic, just like the single exchange interaction in the reference molecule **4**$^{2\bullet}$. It is impossible, however, to draw antiparallel arrows along each of the six edges of the V_4 tetrahedron. This is a three-dimensional extension of the situation encountered in an equilateral triangle of spin centers for which spin frustration has been discussed extensively.[4a,5,14a,17−21] In other words, not all conceivable energetically favorable antiferromagnetic pairwise interactions can be realized in the tetrahedral tetraradical **3**$^{4\bullet}$ simultaneously. Therefore, the effective *J* value, which governs the $\chi-T$ curve, is smaller for the spin-frustrated species **3**$^{4\bullet}$ compared to the value for the diradical **4**$^{2\bullet}$. The most obvious manifestation of this gradation is the fact that for **3**$^{4\bullet}$, in contrast to **4**$^{2\bullet}$, down to the lowest attainable temperature (1.8 K) no

(15) Lyssenko, K. A.; Antipin, M. Y.; Ketkov, S. Y. *Russ. Chem. Bull. Int. Ed.* **2001**, *50*, 130.

(16) (a) Crawford, V. H.; Richardson, H. W.; Wasson, J. R.; Hodgson, D. J.; Hatfield, W. E. *Inorg. Chem.* **1976**, *15*, 2107. (b) Hodgson, D. J. *Prog. Inorg. Chem.* **1975**, *19*, 173. (c) Nanda, K. K.; Thompson, L. K.; Bridson, J. N.; Nag, K. *J. Chem. Soc., Chem. Commun.* **1994**, 1337.

(17) Woo, H. Y.; So, H.; Pope, M. T. *J. Am. Chem. Soc*. **1996**, *118*, 621.

(18) Cannon, R. D.; White, R. P. *Prog. Inorg. Chem*. **1988**, *36*, 195.

(19) Pavlishchuk, V. V.; Gavrilenko, K. S.; Kolotilov, S. V. *Theor. Exp. Chem.* **2002**, *38*, 21.

(20) McCusker, J. K.; Vincent, J. B.; Schmitt, E. A.; Mino, M. L.; Shin, K.; Coggin, D. K.; Hagen, P. M.; Huffman, J. C.; Christou, G.; Hendrickson, D. N. *J. Am. Chem. Soc*. **1991**, *113*, 3012.

(21) McCusker, J. K.; Christmas, C. A.; Hagen, P. M.; Chadha, R. K.; Harvey, D. F.; Hendrickson D. N. *J. Am. Chem. Soc*. **1991**, *113*, 6114.

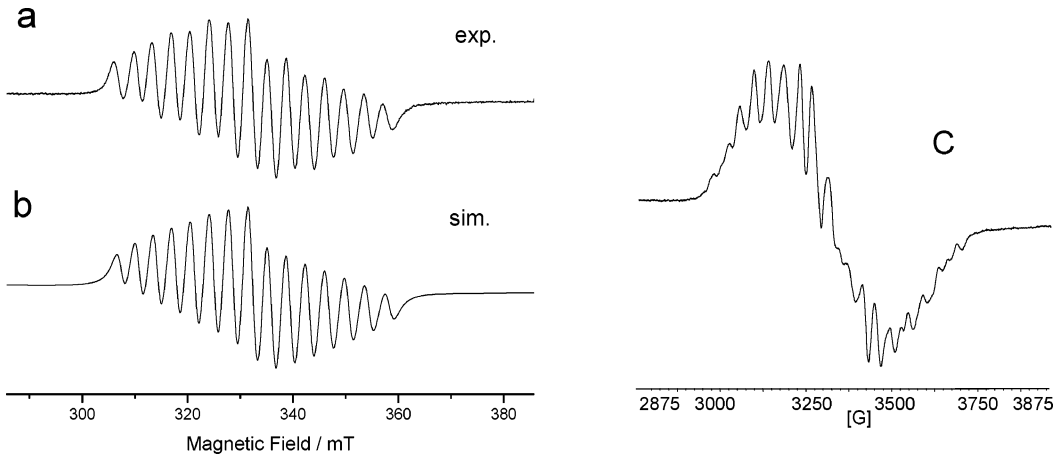

Figure 3. EPR spectra (X-band, $\nu = 9.2166$ GHz) of the diradical $\mathbf{4}^{2\bullet}$ in THF: (a) fluid solution, $T = 300$ K; (b) simulated spectrum, $g = 1.980$, $a(^{51}\mathrm{V}) = 7.25$ mT, $|J| = 1.4$ cm^{-1}; (c) rigid solution, $T = 131$ K, $\nu = 9.2174$ GHz, No $\Delta m_s = 2$ signal was observed.

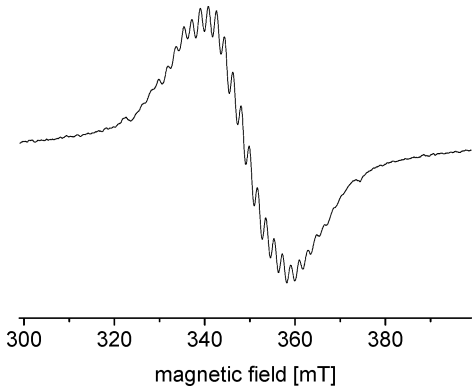

Figure 4. EPR spectrum (X-band, $\nu = 9.6720$ GHz) of the tetraradical $\mathbf{3}^{4\bullet}$ in THF: fluid solution, $T = 300$ K, $g = 1.982$. No $\Delta m_s = 2-4$ signals were observed in the rigid solution spectrum.

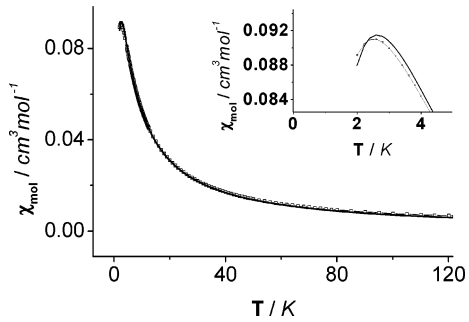

Figure 5. Magnetic susceptibility data for $\mathbf{4}^{2\bullet}$ at 10 kG in the temperature range 1.8−150 K. The solid line represents the best fit to the Bleaney−Bowers expression (see text) with $g = 1.984$, $J_\chi = -2.56(2)$ K, and $\Theta = -3.08(1)$ K.

maximum of the $\chi-T$ curve is detected. The decrease in effective J on going from an organometallic diradical to the corresponding triradical of equilateral triangular structure has been observed previously, as demonstrated by the pairs $\mathbf{6}^{2\bullet}/\mathbf{7}^{3\bullet}$,[22] $\mathbf{8}^{2\bullet}/\mathbf{9}^{3\bullet}$,[5] and $\mathbf{10}^{2\bullet}/\mathbf{11}^{3\bullet}$.[4]

The $\chi-T$ curves for the species $\mathbf{6}^{2\bullet}-\mathbf{11}^{3\bullet}$ of Scheme 2 had been fitted by employing the appropriate equation for two- and three-electron spins engaged in magnetic exchange. Why has this procedure not been applied to the tetraradical $\mathbf{3}^{4\bullet}$? The general approach to derive an equation which describes the

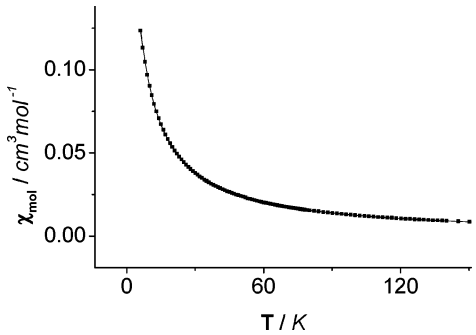

Figure 6. Magnetic susceptibility data for $\mathbf{3}^{4\bullet}$ at 30 kG in the temperature range 1.8−300 K. The solid line represents the best fit to the Curie−Weiss law with $\mu_B = 1.622(1)$, $\Theta = -4.6$ K, and $n = 4$.

temperature dependence of magnetic susceptibility of a tetrahedral tetraradical would proceed as follows.[10e,23,24] The isotropic Heisenberg Hamiltonian[25] $\hat{H} = -2\sum_{j>i=1}^{4} J_{ij}\hat{S}_i\hat{S}_j$ in the most general case of an distorted tetrahedron of C_1 symmetry must include six nonequivalent exchange coupling constants J_{ij}, as six inequivalent pairwise interactions exist.

Four $S = {}^1/_2$ centers give rise to $2^4 = 16$ microstates (M_{S1}, M_{S2}, M_{S3}, $M_{S4} = \pm{}^1/_2$). Therefore, a 16×16 spin matrix under the Heisenberg Hamiltonian specified above must be diagonalized to yield the eigenstates (one quintet, $S_T = 2$; three triplets, $S_T = 1$; two singlets, $S_T = 0$). The energy levels $E(S_T)$ are composite functions of all J_{ij} parameters. Inserting these eigenvalues into the van Vleck equation furnishes the required formula for the temperature dependence of the magnetic susceptibility χ, which is used for fitting the experimental data. Even if a twofold axis (symmetry C_2[10d]) or a mirror plane (symmetry C_s[26]) is retained, the $\chi-T$ formulas for four interacting $S = {}^1/_2$ ions are very extensive. Still higher complexity is

(22) Fieselmann, B. F.; Hendrickson, D. N.; Stucky, G. D. *Inorg. Chem.* **1978**, *17*, 1841.

(23) The derivation of a $\chi-T$ expression for the general case of a tetranuclear complex with $S_1 = S_2 = S_3 = S_4 = {}^1/_2$ and six inequivalent J_{ij} values is outlined in: Sinn, E. *Coord. Chem. Rev.* **1970**, *5*, 313.

(24) (a) Kortz, U.; Nellutla, S.; Stowe, A. C.; Dalal, N. S.; Van Tol, J.; Bassil, B. S. *Inorg. Chem.* **2004**, *43*, 144. (b) Nellutla, S.; van Tol, J.; Dalal, N. S.; Bi, L. H.; Kortz, U.; Keita, B.; Nadjo, L.; Khitrov, G. A.; Marshall, A. G. *Inorg. Chem.* **2005**, *44*, 9795.

(25) In the presence of zero-field splitting (ZFS) the anisotropic terms $D(\hat{S}_z^2 - {}^1/_3\hat{S}^2) + E(\hat{S}_x^2 - \hat{S}_y^2)$ would have to be added to the exchange Hamiltonian. For oligoradicals derived from trovacene units ZFS is not included, as dipolar contributions are negligible because of the large interspin distance (6.4 ± 0.4 Å) and spin−orbit coupling is ineffective due to the ground state A_1 of trovacene. Note the small g anisotropy $\Delta g_{\parallel,\perp}(\mathbf{1}^{\bullet}) \approx 0.03$.

(26) Escuer, A.; Peñalba, E.; Vicente, R.; Solans X.; Font-Bardía, M. *J. Chem. Soc., Dalton Trans.* **1997**, 2315.

Scheme 2

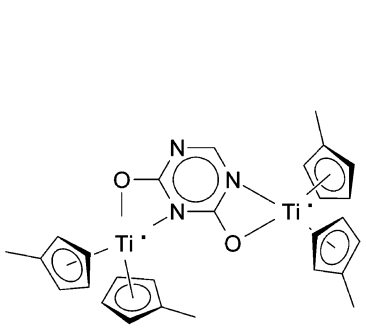

J_χ ($\mathbf{6}^{2\bullet}$) = -2.25 cm^{-1}

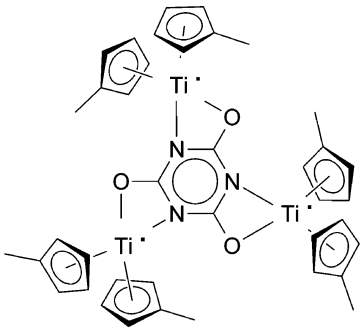

J_χ ($\mathbf{7}^{3\bullet}$) = -0.93cm^{-1}

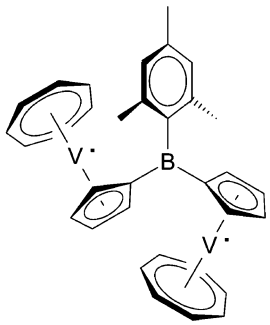

J_χ ($\mathbf{8}^{2\bullet}$) = -0.96 cm^{-1}

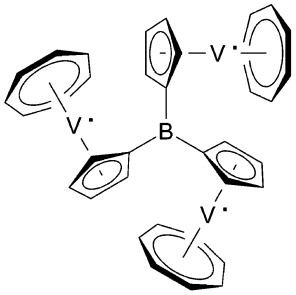

J_χ ($\mathbf{9}^{3\bullet}$) = -0.35 cm^{-1}

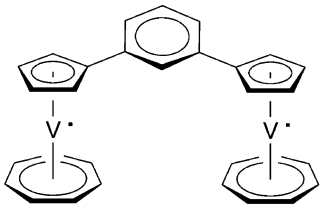

J_χ ($\mathbf{10}^{2\bullet}$) = -1.67 cm^{-1}

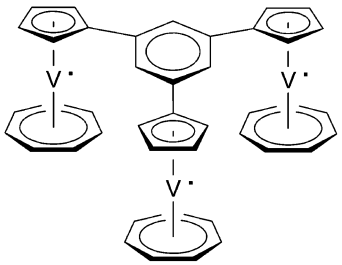

J_χ ($\mathbf{11}^{3\bullet}$) = -0.68 cm^{-1}

expected for C_1 symmetry, as encountered in $\mathbf{3}^{4\bullet}$. Aggravating this situation is the fact that in the crystal two forms of $\mathbf{3}^{4\bullet}$ with differing tetrahedral angles at the central tin atoms are present. This brings the number of J_{ij} parameters to 12; the number of fit parameters would become even higher if, as is customary, corrections for the presence of a paramagnetic impurity and for intermolecular exchange interactions were included. Therefore, attempts to simulate the (relatively featureless) $\chi-T$ curve of $\mathbf{3}^{4\bullet}$ appear futile, as several independent sets of parameters may exist which reproduce the susceptibility curve.[23,27] Furthermore, unequivocal assignment of individual J_{ij} values to V_iV_j pairs, a requirement for magnetostructural correlations, would be impossible. Thus, while the existence of intramolecular magnetic exchange interaction of the four V(d^5) atoms in $\mathbf{3}^{4\bullet}$ is firmly established by the EPR spectra in dilute fluid solution, quantitative determination of the exchange coupling constants J_{ij} from magnetic susceptibility data is impractical.

Cyclic Voltammetry. Apart from magnetocommunication the complexes $\mathbf{4}^{2\bullet}$ and $\mathbf{3}^{4\bullet}$ should also engage in electrocommunication, which expresses itself in redox splitting: i.e., the difference of potentials characterizing subsequent redox steps. The cyclic voltammograms for $\mathbf{4}^{2\bullet}$ and $\mathbf{3}^{4\bullet}$ are presented in Figure 7; relevant data are collected in the caption. Discussion of electrochemical results on $\mathbf{4}^{2\bullet}$ and $\mathbf{3}^{4\bullet}$ benefits from comparison with those for ferrocenylsilanes.[7] Since use of the solvent benzonitrile was reported to improve the resolution of successive waves, we adopted this medium as well.

For tetrakis([5]trovacenyl)tin ($\mathbf{3}^{4\bullet}$) in the region of trovacene oxidation a barely resolved four-electron wave is observed with a total spread of 270 mV. Three out of the four expected constituent waves are clearly seen; the fourth inflection is hidden under a correspondingly larger potential step. Whereas it would be pretentious to discuss small differences in the redox splittings, it is remarkable that the mean splitting $\delta E_{1/2}$ = 90 mV falls short of that observed for tetrakis(ferrocenyl)-silicon ($\delta E_{1/2}$ = 140 mV).[7] Taking into consideration that the redox orbital is essentially metal centered (V $3d_{z^2}$), the gradation of $\delta E_{1/2}$ values is plausible on electrostatic grounds in view of the larger intervanadium distance of 6.4 ± 0.4 Å in tetra([5]trovacenyl)tin compared to 5.7 ± 0.4 Å in tetrakis-(ferrocenyl)silicon. Furthermore, since for π-perimeter coordination the $M\xrightarrow{\delta}C_nH_n$ back-bonding ability increases in the series C_5H_5 < C_6H_6 < C_7H_7,[28] in the unsymmetrical sandwich complex trovacene central metal oxidation will diminish V

(27) (a) Ruiz, E.; Rodríguez-Fortea, A.; Cano, J.; Alvarez, S.; Alemany, P. *J. Comput. Chem.* **2003**, *24*, 982. (b) Ruiz, R.; Alvarez, S.; Rodríguez-Fortea, A.; Alemany, P.; Pouillon, Y.; Massobrio, C. In *Magnetism: Molecules to Material II*; Miller, J. S., Drillon, M., Eds.; Wiley-VCH,: Weinheim, Germany, 2001; Chapter 7.

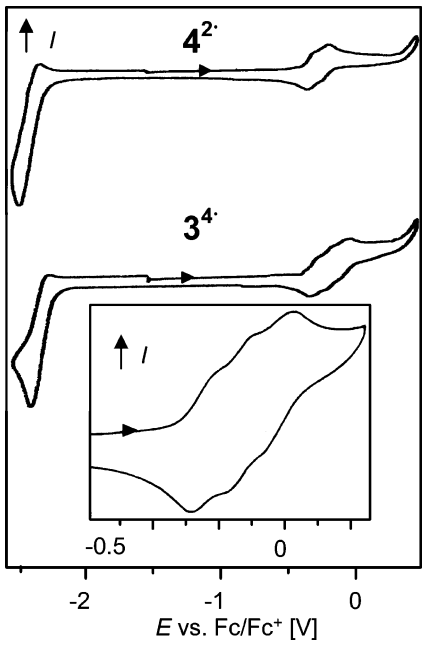

Figure 7. Cyclic voltammetry traces for the complexes $\mathbf{3}^{4\bullet}$ and $\mathbf{4}^{2\bullet}$ (C_6H_5CN, 0.1 M $(n\text{-Bu})_4NClO_4$, $T = -25$ °C, $\nu = 100$ mV s^{-1}, glassy-carbon working electrode, E vs ferrocene/ferrocenium couple). The inset displays a expansion of the oxidation wave region of $\mathbf{3}^{4\bullet}$. $\mathbf{3}^{4\bullet}$: $E_{1/2}(n-/0) = -2.278$ V, $\Delta E_p = 148$ mV; $E_{1/2}(0/+) = -0.241$ V, $\Delta E_p = 70$ mV; $E_{1/2}(+/2+) = -0.140$ V, $\Delta E_p = 64$ mV; $\delta E_{1/2}(0/+/2+) = 101$ mV; $E_{1/2}(2+/3+) = -0.022$ V, $\Delta E_p = 64$ mV; $\delta E_{1/2}(+/2+/3+) = 118$ mV. $\mathbf{4}^{2\bullet}$: $E_{1/2}(n-/0) = -2.275$ V, $\Delta E_p = 142$ mV; $E_{1/2}(0/+) = -0.202$ V, $\Delta E_p = 72$ mV; $E_{1/2}(+/2+) = -0.110$ V, $\Delta E_p = 64$ mV, $\delta E_{1/2}(0/+/2+) = 92$ mV.

$\overset{\delta}{\rightarrow}C_7H_7$ back-bonding to a larger extent than $V\overset{\delta}{\rightarrow}C_5H_5$ back-bonding. This will shift an increment of positive partial charge into the peripheral C_7H_7 ligand, again decreasing intramolecular electron repulsion and thereby the redox splitting $\delta E_{1/2}$.

By way of conclusion it may be stated that tin as a spacer atom mediates magnetocommunication less extensively than carbon or silicon. Exchange coupling in tetrakis([5]trovacenyl)-tin ($\mathbf{3}^{4\bullet}$) falls short of that observed for bis([5]trovacenyl)-diphenyltin ($\mathbf{4}^{2\bullet}$). In $\mathbf{3}^{4\bullet}$ competing interactions of opposite sign and/or spin frustration are thought to operate. With regard to electrocommunication redox splitting shows the gradation $\delta E_{1/2}$[tetrakis([5]trovacenyl)Sn] < $\delta E_{1/2}$[tetrakis(ferrocenyl)Si].

Experimental Section

All chemical manipulations were performed under an atmosphere of purified dinitrogen or argon in dried and degassed solvents, employing standard Schlenk techniques. Physical measurements were carried out with instruments specified previously.[4b]

X-ray Structure Determination of $\mathbf{3}^{4\bullet}$ and $\mathbf{4}^{2\bullet}$. All data were collected at low temperatures on a Stoe IPDS-II diffractometer employing Mo Kα radiation ($\lambda = 0.710\ 73$ Å). The structures were solved by direct methods (SHELXS-97) and refined on F^2 values using a full-matrix least-squares procedure, and all non-hydrogen atoms were refined anisotropically. Hydrogen atoms were included at calculated positions and refined on the basis of a riding model.

Crystal data for $\mathbf{3}^{4\bullet}$: $C_{51.50}H_{48}SnV_4$, $M_r = 989.35$, crystal size 0.39 × 0.23 × 0.06 mm3, triclinic, space group $P\bar{1}$, $Z = 4$, $a =$ 13.7723(6) Å, $b = 16.9996(7)$ Å, $c = 18.7871(8)$ Å, $\alpha = 69.348(3)°$, $\beta = 83.322(3)°$, $\gamma = 78.093(3)°$, $V = 4022.7(3)$ Å^3, $d_{calcd} = 1.634$ Mg m^{-3}, absorption coefficient 1.544 mm^{-1}, $F(000) = 1996$, $T = 193(2)$ K, θ range 1.61−27.03°, index ranges $-17 \le h \le 17$, $-21 \le k \le 21$, $-23 \le l \le 23$, 64 002 reflections collected, 17 502 independent reflections (R(int) = 0.0391), 13 772 observed reflections ($I > 2\sigma(I)$), 17 502 reflections used for refinement, largest difference peak and hole 0.565 and −0.670 e Å^{-3}, goodness of fit on F^2 0.975, R index (all data) wR2 = 0.0657, R index conventional ($I > 2\sigma(I)$) R1 = 0.0268.

Crystal data for $\mathbf{4}^{2\bullet}$: $C_{36}H_{32}SnV_2$, $M_r = 685.19$, crystal size 0.48 × 0.21 × 0.05 mm^3, triclinic, space group $P\bar{1}$, $Z = 2$, $a = 9.3888(11)$ Å, $b = 11.7664(15)$ Å, $c = 13.4341(16)$ Å, $\alpha = 80.247(10)°$, $\beta = 82.341(10)°$, $\gamma = 78.299(10)°$, $V = 1424.7(3)$ Å^3, $d_{calcd} = 1.597$ Mg m^{-3}, absorption coefficient 1.536 mm^{-1}, $F(000) = 688$, $T = 193(2)$ K, θ range 1.55−24.95°, index ranges $-11 \le h \le 11$, $-13 \le k \le 13$, $-15 \le l \le 15$, 12 471 reflections collected, 4942 independent reflections ($R_{int} = 0.0401$), 4324 observed reflections ($I > 2\sigma(I)$), 4942 reflections used for refinement, largest difference peak and hole 0.757 and −0.375 e Å^{-3}, goodness of fit on F^2 0.972, R index (all data) wR2 = 0.0527, R index conventional ($I > 2\sigma(I)$) R1 = 0.0213.

[(η^7-C_7H_7)V(η^5-C_5H_4)]$_4$Sn ($\mathbf{3}^{4\bullet}$). Solutions of trovacene ($\mathbf{1}^{\bullet}$; 1.07 g, 5.17 mmol) in diethyl ether (150 mL) and *n*-butyllithium (3.23 mL 1.6 M in hexane, 5.17 mmol) were combined and stirred for 12 h at room temperature. After the mixture was cooled to 0 °C, $SnCl_4$ (0.09 mL, 0.66 mmol) was added dropwise over 30 min. After this mixture was stirred at room temperature for 1 h, more $SnCl_4$ (0.09 mL, 0.66 mmol) was added to the suspension, immediately affording a large amount of yellow precipitate. The mixture was allowed to react overnight at ambient temperature. After filtering, washing with diethyl ether, and drying in vacuo the yellow solid was extracted with 30 mL of THF/CH_2Cl_2 (1/3). This extract was filtered through a short column of Al_2O_3 (2 × 6 cm) and the filtrate again taken to dryness. Final purification proceeded by column chromatography (Al_2O_3, 1 × 20 cm), residual $\mathbf{1}^{\bullet}$ was eluted by toluene/petroleum ether (1/1) and the product $\mathbf{3}^{4\bullet}$ by THF/toluene. Tetra([5]trovacenyl)tin ($\mathbf{3}^{4\bullet}$) was obtained as a pale purple solid (250 mg, 22%). Crystals for X-ray diffraction were grown from THF/toluene/Et_2O at 8 °C. EI-MS (70 eV): *m*/*z* 944 (8%, $M^+ + 1$), 737 (5%, $(C_{12}H_{11}V)_3Sn^+$), 531 (5%, $(C_{12}H_{11}V)_2Sn^+$), 319 (20%, $C_{12}H_{11}VSn^+$), 207 (100%, $C_{12}H_{12}V^+$). Anal. Calcd for $C_{48}H_{24}SnV_4$ (942.93): C, 61.13; H, 4.67. Found: C, 60.94; H, 5.12. For EPR and CV data see text.

[(η^7-C_7H_7)V(η^5-C_5H_4)]$_2$(C_6H_5)$_2$Sn ($\mathbf{4}^{2\bullet}$). To a solution of (C_7H_7)V(C_5H_4Li) prepared from $\mathbf{1}^{\bullet}$ (742 mg, 3.58 mmol) in 100 mL of diethyl ether and *n*-butyllithium (2.3 mL, 1.6 M in hexane, 3.68 mmol) was added (C_6H_5)$_2SnCl_2$ (615 mg, 1.79 mmol). Stirring overnight at room temperature afforded a purple suspension. Solid LiCl was removed by filtration, and the filtrate was freed from solvent in vacuo. The crude product was purified by column chromatography (2 × 20 cm, Al_2O_3, 1/1 toluene/Et_2O). Bis([5]-trovacenyl)diphenyltin ($\mathbf{4}^{2\bullet}$) was obtained as a purple solid (260 mg, yield 21%). EI-MS (70 eV): *m*/*z* 687 (9%, $M^+ + 2$), 685 (6%, M^+), 207 (67%, $C_{12}H_{11}V^+$), 129 (41%, $C_6H_6V^+$), 116 (29%, $C_5H_5V^+$), 91 (100%, $C_7H_7^+$). Anal. Calcd for $C_{36}H_{32}SnV_2$ (684.93): C, 63.12; H, 4.67. Found: C, 61.88; H, 4.88. For EPR and CV data see text.

Acknowledgment. This work was supported by the "Deutsche Forschungsgemeinschaft" and the "Fonds der Chemischen Industrie".

Supporting Information Available: CIF files giving crystal data for $\mathbf{3}^{4\bullet}$ and $\mathbf{4}^{2\bullet}$. This material is available free of charge via the Internet at http://pubs.acs.org.

OM700300J

(28) Elschenbroich, C. *Organometallics*, 3rd ed.; Wiley-VCH: Weinheim, Germany, 2006; p 552.